Binding of SSB and RecA Protein to DNA-Containing Stem Loop Structures: SSB Ensures the Polarity of RecA Polymerization on Single-Stranded DNA†

M. Sreedhar Reddy, Moreshwar B. Vaze, K. Madhusudan, and K. Muniyappa*

Department of Biochemistry, Indian Institute of Science, Bangalore 560 012, India

Received May 24, 2000; Revised Manuscript Received August 16, 2000

ABSTRACT: Single-stranded DNA-binding proteins play an important role in homologous pairing and strand exchange promoted by the class of RecA-like proteins. It is presumed that SSB facilitates binding of RecA on to ssDNA by melting secondary structure, but direct physical evidence for the disruption of secondary structure by either SSB or RecA is still lacking. Using a series of oligonucleotides with increasing amounts of secondary structure, we show that stem loop structures impede contiguous binding of RecA and affect the rate of ATP hydrolysis. The electrophoretic mobility shift of a ternary complex of SSB−DNA−RecA and a binary complex of SSB−DNA are similar; however, the mechanism remains obscure. Binding of RecA on to stem loop is rapid in the presence of SSB or ATPγS and renders the complex resistant to cleavage by *HaeIII*, to higher amounts of competitor DNA or low temperature. The elongation of RecA filament in a 5′ to 3′ direction is halted at the proximal end of the stem. Consequently, RecA nucleates at the loop and cooperative binding propagates the RecA filament down the stem causing its disruption. The pattern of modification of thymine residues in the loop region indicates that RecA monomer is the minimum binding unit. Together, these results suggest that SSB plays a novel role in ensuring the directionality of RecA polymerization across stem loop in ssDNA. These observations have fundamental implications on the role of SSB in multiple aspects of cellular DNA metabolism.

Single-stranded DNA is a transient intermediate in most aspects of DNA metabolism including DNA replication, repair, and recombination (reviewed in refs *1* and *2*). Data from genetic studies as well as biochemical and structural analyses is consistent with the notion that these processes entail the interconversion of DNA between duplex and single-stranded forms. Furthermore, recent data from human genetic studies and from model organisms suggest that trinucleotide repeats expansion diseases arise, at least in part, from improper secondary structure (reviewed in ref *3*). Genetic studies indicate that expansion diseases might result from the failure of replication/repair enzymes to traverse and disrupt stem loop structures (*3*).

Escherichia coli single-stranded DNA-binding protein (SSB)[1] is a prominent member of a family of proteins that play a central role in DNA replication, repair of damaged DNA and homologous recombination (*1*, *2*). The multiple phenotypes displayed by *E. coli* strains bearing mutations in the *ssb* gene are indicative of its essential role in various aspects of DNA metabolism. These include cessation of DNA replication, reduced recombination, and failure to activate SOS response (*4*−*6*). SSB exits as a stable homotetramer, each of which contains a binding site for an octanucleotide (*7*−*9*). The tetrameric structure remains intact when it binds ssDNA. Other studies have established a complex web of interactions between SSB and ssDNA. Using fluorescence and hydrodynamic measurements, Lohman and his colleagues have demonstrated at least three distinct binding modes as $(SSB)_n$, $n = 35$, 56, and 65 nucleotides/SSB tetramer (reviewed in ref *1*). The binding site size of *E. coli* SSB is influenced, in a qualitative and quantitative manner, by solution variables such as pH, temperature, monovalent and divalent cations, anions, and binding density (*10*−*14*). Visualization of SSB−ssDNA complexes by electron microscopy indicates that the binding modes of SSB correspond to different morphologies of DNA−protein lattice (*15*). The $(SSB)_{56}$/$(SSB)_{65}$ binding mode formed in solutions containing high salt and lower binding densities display "limited" cooperativity and a "beaded" appearance to ssDNA. The $(SSB)_{35}$ mode formed in solutions containing low salt and higher binding density confers "unlimited" cooperativity and "smooth" appearance to ssDNA (*1*, *15*, *16*). The transition between the two binding modes is reversible and modified by the solution variables. It has been proposed that different binding modes may be used selectively for different processes such as DNA replication, recombination and repair (*1*).

Corresponding SSBs from several other systems have also been characterized and similarly implicated in DNA metabolism (reviewed in ref *17*). Although the mechanism of action of *E. coli* SSB has been phylogenetically conserved, the demands of DNA metabolism in eukaryotes are met by a heterotrimeric RPA complex, composed of 70-, 32-, and 14-kDa subunits. Several lines of evidence suggest that all of the subunits are essential for function (*17*). RPA interacts

† This work was funded in part by a grant from the Wellcome Trust, England, and from the Council of Scientific and Industrial Research, New Delhi, India, to K.M.

* To whom correspondence should be addressed. Phone: (+91-80) 309 2235. Fax: (+91 80) 360 0814/0683. E-mail: kmbc@biochem.iisc.ernet.in.

[1] Abbreviations: BSA, bovine serum albumin; DTT, dithiotreitol; RecA, RecA protein of *Escherichia coli*; SSB, single-stranded DNA-binding protein of *E. coli*; SSBs, single-strand binding proteins; ATPγS, adenosine 5′-*O*-(thiotriphosphate); ssDNA, single-stranded DNA; T, thymine.

10.1021/bi001187+ CCC: $19.00
Published on Web 10/24/2000

Table 1: Oligonucleotides Used in This Study

substrate	sequence (5′ to 3′)[a]	length (bases)	ΔG (kcal mol^{-1})
GC702	GCCACGTGCGTGCCGC**GTGGCCCG**TCTC **CGGGCCAC**TGCTGCGATGAGCCGC	52	−14.7
GC701	GCCACGTGCGTGCCGC**GTGGCCTA**TCTC **TAGGCCAC**TGCTGCGATGAGCCGC	52	−10.6
GC703	GCTGCGTGCGTGCCGCGT**GGCCTA**TCTC **TAGGCC**GTTGCTGCGATGAGCCGC	52	−7.4
GC704	GCTGCGTGCGTGCCGCGT**GGCCT**GTCTCT **AGGCC**GTTGCTGCGATGAGCCGC	52	−6.6
GC705	GCTGCGTGCGTGCCGCGT**AGCCT**GTCTCT **AGGCT**GTTGCTGCGATGAGCCGC	52	−5.1
GC30	ACTATGTATGTACTATGACTATAATACTAT GATGAGCTAC	40	0.0

[a] Nucleotide residues shown in boldface can fold into stem loop configuration.

with a number of components of DNA metabolism in the cell. For example, RPA is required for the initiation of SV 40 DNA replication, excision repair (XPA and XPG), and homologous recombination (Rad51 and Rad52) and has been proposed to link transcription to DNA replication through its interaction with Gal4, VP16, and p53 (reviewed in ref *17*).

Both genetic and biochemical studies indicate that *E. coli* SSB influences the activities of its cognate RecA and RecBCD proteins (reviewed in refs *18*−*20*). However, the mechanism by which SSB stimulates the activities of RecA is not clear and is subject of debate. SSB plays a crucial role in both homologous pairing as well as strand exchange promoted by RecA. The active form of RecA is the nucleoprotein filament where the protein binds cooperatively around ssDNA. It has been conjectured that SSB facilitates the formation of nucleoprotein filaments of RecA−ssDNA by its ability to melt out secondary structure (*22*−*24*). Depending on the order of incubation of SSB with ssDNA in relation to RecA, and the method of assay used for quantification, differences in the stoichiometric ratios of SSB and RecA have been noted (reviewed in refs *18*−*20*). Some studies have shown continuous association of stoichiometric ratios of SSB with the nucleoprotein filament of RecA (*16*, *21*), while others have observed that binding of RecA and SSB to ssDNA is mutually exclusive (*23*, *24*).

In four-strand exchange, a distinct role for SSB is obscure. However, the pairing of circular DNA with extended length of gaps and linear duplex DNA require the participation of SSB (*25*). Likewise, SSB helps in postsynaptic phase of three-strand exchange by sequestering the 5′ end of the displaced ssDNA, and thereby inhibits its participation in additional pairing reactions (*26*, *27*). The interaction of RecA with ssDNA containing increasing amounts of secondary structure has not been investigated thoroughly. Moreover, there has been no physical evidence for intramolecular base pairing disruption by either SSB or RecA. Consequently, the paths of disruption of stem loop by these proteins remain unknown. Using a series of oligonucleotide substrates containing increasing amounts of secondary structure, we provide evidence for the ability of RecA and SSB to disrupt stem loop structures. Significantly, these results disclose a novel role for SSB in ensuring the polarity of RecA polymerization on ssDNA containing stem loop structures.

EXPERIMENTAL PROCEDURES

Reagents, DNA, and Proteins. All chemicals are of reagent grade. Buffers were made using deionized water. ATP, ATPγS, NADH, pyruvate kinase, and lactate dehydrogenase were purchased from Boehringer Mannheim, Germany. Phage T4 polynucleotide kinase and *HaeIII* were obtained from New England Biolabs. Single-stranded oligonucleotides were purchased from Life Technologies, New York. Oligonucleotides containing expected amounts of secondary structure were designed using the GCG software package (Genetic Computer Group, University of Wisconsin, Madison, WI). Oligonucleotides were purified in 15% polyacrylamide gels containing 8 M urea, eluted from acrylamide with 10 mM Tris-HCl (pH 7.5) containing 1 mM EDTA, and their concentration was estimated using the ϵ_{260} provided by the manufacturer. Purified oligonucleotides were stored as 500 μM stock solutions in 10 mM Tris-HCl buffer (pH 7.5) containing 1 mM EDTA at −20 °C. The formation and thermodynamic parameters of hairpins was ascertained by UV spectroscopy as described (*28*). Table 1 shows the sequences of oligonucleotide substrates with secondary structure ranging from $\Delta G = -5.1$ through −14.7 kcal mol^{-1}. Oligonucleotides were labeled at the 5′ ends using [γ-^{32}P]ATP and phage T4 polynucleotide kinase (*29*). Free ATP was removed by gel filtration using a Sephadex G50 column (*29*). Circular single-stranded DNA from phage M13 was prepared as described (*30*). DNA concentrations are expressed as total nucleotide residues. RecA (*31*) and SSB (*32*) from *E. coli* were purified, and their concentration was determined as described (*33*). Monoclonal antibodies to RecA and SSB were prepared, characterized, and used as described (*16*). ^{35}S-labeled RecA and SSB proteins were purified as described (*33*).

ATPase Assay. ATP hydrolysis catalyzed by RecA was measured by coupled enzymatic assay in a spectrometer as described (*24*). The assay buffer (0.5 mL) contained 20 mM Tris-HCl (pH 7.5), 12 mM $MgCl_2$, 1 mM DTT, 1.5 mM ATP, 6 mM phosphoenol pyruvate, 0.1 mg/mL NADH, 1.2 μM DNA (M13 ssDNA or oligonucleotide), and 12.5 units each of pyruvate kinase and lactate dehydrogenase per reaction. Samples were preincubated at 37 °C for 2 min in a Shimadzu spectrophotometer equipped with temperature control and recording attachments. The reaction was initiated by the addition of 0.8 μM RecA protein. Following the decrease in absorbency at 340 nm, we monitored the progress of the reaction over a period of 30 min. Rates of the reaction was calculated from the slope of the curve.

Electrophoretic Mobility Shift Assays. The assay was performed as described (*34*). Assay buffer (20 μL) contained 30 mM Tris-HCl (pH 7.5), 12 mM $MgCl_2$, 0.1 mM ATPγS,

1. 4 mM DTT, 3 μM ^{32}P-labeled oligonucleotide, 1 μM RecA and 100 μg/mL BSA and 0.2 μM SSB, where mentioned. Reactions were performed at 37 °C for 15 min in the following order: 5 min with SSB followed by 10 min with RecA. Reactions were terminated by the addition of 3 μL of loading buffer [20% glycerol containing 0.12% (w/v) each of bromophenol blue and xylene cyanol]. Samples were loaded onto a 8% polyacrylamide gel, electrophoresed at 4 °C in 13.2 mM Tris-acetate (pH 7.4) at 12 V/cm for 4 h. The gel was dried on a Whatman 3MM filter paper and visualized by autoradiography. Samples containing RecA−DNA or SSB−DNA complexes were incubated with affinity purified anti-RecA (5.8 μM) or anti-SSB (0.2 μM) antibody for an additional 5 min. Samples were analyzed by polyacrylamide gel electrophoresis as described above.

Binding of RecA and SSB to Stem Loop as Monitored by Protection from HaeIII Cleavage. Reaction mixture (20 μL) contained 30 mM Tris-HCl (pH 7.5), 12 mM $MgCl_2$, 0.1 mM ATPγS or 1 mM ATP, 1. 4 mM DTT, 3 μM ^{32}P-labeled 52-mer DNA ($\Delta G = -10.6$), 1 μM RecA, and 100 μg/mL BSA. The reaction mixtures were incubated at 37 °C for the indicated time periods followed by the addition of 10 units *HaeIII*. Reactions were continued for 30 min and were stopped by the addition of EDTA to a final concentration of 50 mM. Extraction of protein and ethanol precipitation of DNA was performed as described (*29*). DNA was resuspended in 10 μL of loading solution containing 80% formamide, 10 mM NaOH, 1 mM EDTA, and 0.1% (w/v) each of bromophenol blue and xylene cyanol. Samples were electrophoresed in 12% polyacrylamide gels in the presence of 8 M urea at 24 °C in 89 mM Tris/borate buffer (pH 8.3) at 12 V/cm for 4 h. In competition assays, ^{32}P-labeled ssDNA−RecA complexes were challenged with the indicated amount of unlabeled DNA. After 30 min incubation, DNA was digested with *HaeIII*, and the products were separated on polyacrylamide gels as described above. The gels were dried and the bands were quantified on a UVItech gel documentation system (England) by using UVIBAND version 97.04 software.

Chemical Modification of Oligonucleotide Substrates with $KMnO_4$. Binary complexes of RecA−DNA or ternary complexes of RecA−ssDNA−SSB were formed as described above except that DTT was omitted. Reaction mixture (40 μL) containing 3 μM ^{32}P-labeled 52-mer DNA, 1 μM RecA, 0.1 mM ATPγS, or 1 mM ATP were incubated for various time periods as indicated. In experiments involving SSB, the reactions were performed under identical conditions containing 0.2 μM SSB. Each sample was treated with 0.1 mM $KMnO_4$ (freshly dissolved in H_2O) or 5 μL of 5% DMS for 2 min at 37 °C. Reaction was stopped by the addition of 5 μL of DMS stop buffer (*35*) and 150 μL of ethanol (−20 °C). DNA was collected by centrifugation, resuspended in 200 μL of 10 mM Tris-HCl (pH 7.5) containing 1 mM EDTA solution, extracted with phenol-chloroform-isoamyl alcohol solution, and precipitated with ethanol. Modified DNA was subjected to cleavage by incubation with 1 M piperidine at 90 °C for 30 min (*35*). Samples were dried, and the pellets were resuspended in 100 μL of H_2O. This procedure was repeated three times. The pellets were dissolved in a solution containing 80% formamide, 10 mM NaOH, and 0.1% each of bromophenol blue and xylene cyanol. The reaction products were separated on a 12% polyacrylamide gel in the presence of 8 M urea that was run at 1800 V for 2 h. The gels were dried and subjected to autoradiography. The bands were analyzed and quantified on a UVItech gel documentation system (England), by using UVIBAND version 97.04 software.

Table 2: Effect of Increasing Amounts of Secondary Structure on the Rate of ssDNA-Dependent ATP Hydrolysis by RecA Protein

		ATPase activity		
substrate	$-\Delta G$ (kcal mol^{-1})	ΔA (min^{-1})	activity (μmol min^{-1})	% M13 ssDNA
none		0.0006	0.10	
M13 ssDNA	NA	0.0306	4. 92	100.0
GC30	0.0	0.033	5.30	107.7
GC705	5.1	0.0284	4.56	92.7
GC703	7.4	0.0208	3.34	67.9
GC701	10.6	0.0152	2.24	48.8
GC702	14.7	0.0109	1.75	35.6

[a] NA, not available.

RESULTS

Experimental Approach. In the experiments described throughout this study, we used oligonucleotide substrates and two principal assays: electrophoretic mobility shift assay and enzymatic and chemical probing methods. Due to its simplicity the former is useful for exploring binding of proteins to DNA and the latter reactions are appropriate to monitor the kinetics of disruption of stem loop in real time. Thus, synthetic model substrates might provide direct evidence for the influence of secondary structure on the DNA-binding activities of both SSB and RecA.

Extent of Inhibition of ATPase Activity of RecA Is Proportional to the Degree of Secondary Structure. To examine the influence of secondary structure on the DNA-binding properties of RecA, we designed a series of 52-mer DNA substrates (Table 1). When the prototypical substrate undergoes folding, it forms a stem loop flanked by a stretch of 16−18 nucleotide residues at both 5′ and 3′ ends. The loop spans 4−6 nucleotide residues, whereas the stem length ranges 5−8 bp. The stem loops in these substrates possess ΔG ranging from −5.1 through −14.7 kcal mol^{-1}. Thus, in this configuration, the presence of ssDNA at both 5′ and 3′ ends ensures the minimal length necessary for the formation of an active nucleoprotein filament of RecA−ssDNA (*36*, *37*).

First, we wished to explore the influence of increasing amounts of secondary structure on the ability of RecA to catalyze ssDNA-dependent ATP hydrolysis by spectrophotometric assay (*24*). As positive controls, we used 40-mer DNA that is devoid of secondary structure and M13 ssDNA. After mixing all of the components in a cuvette and preincubation, the reaction was initiated by the addition of 1.5 mM ATP. As reported previously, ssDNA-dependent ATPase activity of RecA had an apparent k_{cat} for ATP hydrolysis of 23 min^{-1}. In contrast, the rate of ATP hydrolysis with ssDNA substrates containing stem loop declined with increasing amounts of secondary structure. Table 2 shows the average rates of ATP hydrolysis derived from quantitative analysis of data from triplicate experiments. These results suggest that inhibition of ATPase activity of RecA arise solely from secondary structure in ssDNA.

Binding of RecA and SSB to ssDNA with Increasing Amounts of Secondary Structure. It has been previously

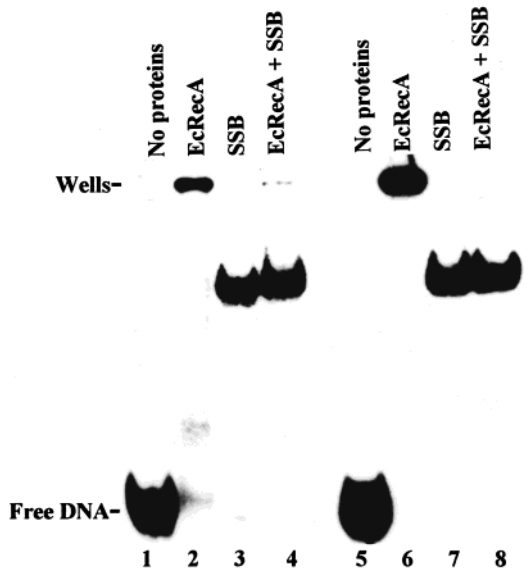

FIGURE 1: Binding of RecA and SSB to ssDNA. Reaction mixtures contained 3 μM ^{32}P-labeled 52-mer DNA (lanes 1−4) containing secondary structure ($\Delta G = -14.7$ kcal mol^{-1}) or 40-mer DNA devoid of secondary structure (lanes 5−8), 0.1 mM ATPγS, 12 mM $MgCl_2$, 1 μM RecA (lanes 2 and 6), 0.2 μM SSB (lanes 3 and 7), or both proteins at the same concentrations (lanes 4 and 8). Samples were incubated at 37 °C for 15 min, separated on a 8% polyacrylamide gel and visualized by autoradiography as described in the Experimental Procedures. The positions of free DNA and wells are indicated.

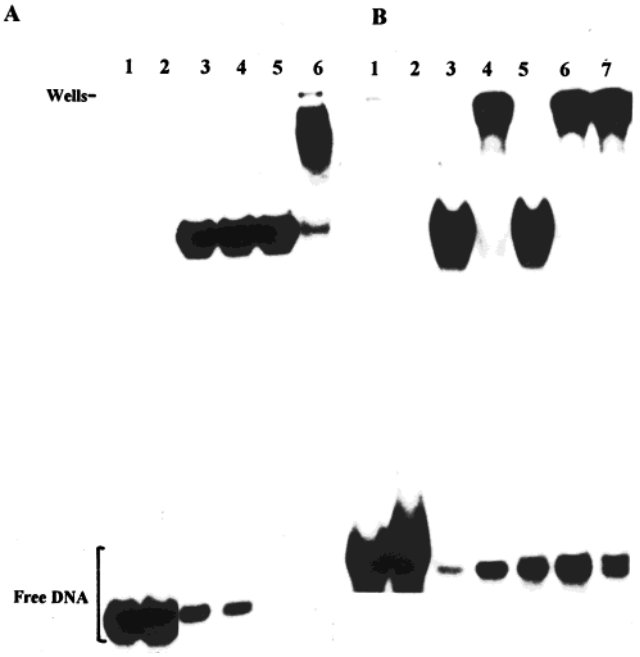

FIGURE 2: Supershift assays confirm the presence of both SSB and RecA in the nucleoprotein filaments. (A) Assay performed with anti-RecA antibodies. Reaction mixtures contained 3 μM ^{32}P-labeled 52-mer DNA ($\Delta G = -14.7$ kcal mol^{-1}), 0.1 mM ATPγS, 12 mM $MgCl_2$ in the absence (lane 1 and 2) or presence of 0.2 μM SSB (lanes 3 and 4) or 1 μM RecA and 0.2 μM SSB (lanes 5 and 6). Following incubation at 37 °C for 15 min, 5.8 μM α-RecA antibody (lanes 2, 4, and 6) or an equal volume of phosphate buffered saline (lanes 1, 3, and 5) were added and incubation was continued for an additional 5 min. Finally, samples were separated on a 8% polyacrylamide gel and visualized by autoradiography as described in the Experimental procedures. (B) Assay was performed as in Figure 2A, but with α-SSB antibodies. Reactions were performed in the absence (lanes 1 and 2) or presence of 0.2 μM SSB (lanes 3 and 4) or with 0.2 μM SSB and RecA at 1 μM (lanes 5 and 6) or 2 μM (lane 7). After incubation for 15 min at 37 °C, samples (lanes 2, 4, 6, and 7) were incubated with an anti-SSB antibody (0.2 μM) or an equal volume of phosphate buffered saline (lanes 1, 3, and 5) for an additional 5 min at 37 °C. Samples were separated on an 8% polyacrylamide gel and visualized by autoradiography as described in the Experimental procedures. These experiments were repeated with substrates containing different amounts of secondary structure with identical results.

demonstrated that binding of RecA or RPA to oligonucleotide substrates can be monitored by electrophoretic mobility shift assays (*34*, *36*, *38*, *39*). To investigate the influence of increasing amounts of secondary structure on the binding of SSB or RecA to ssDNA, we carried out electrophoretic mobility shift assays with ^{32}P-labeled ssDNA substrates. The binding of RecA or SSB, and both proteins to ^{32}P-labeled DNA was performed in an assay buffer containing 12 mM Mg^{2+} and 0.1 mM ATPγS. Protein−DNA complexes were separated on polyacrylamide gels and visualized by autoradiography. Data in Figure 1 (lanes 1−4) shows the results of a representative autoradiogram of an assay performed with 52-mer DNA ($\Delta G = -14.7$ kcal mol^{-1}), RecA, and ATPγS. Under these conditions, RecA formed complexes with broad structural heterogeneity, and a significant portion of them did not migrate beyond the origin of the gel. By contrast, SSB bound the same substrate efficiently forming a discrete protein−DNA complex. Intriguingly, incubation of both the proteins produced a discrete protein−DNA complex similar in size with that formed with SSB alone. Similar results were also observed with oligonucleotides containing increasing amounts of secondary structure that were incubated solely with RecA, SSB, or both proteins (data not shown). To ascertain that the differences observed were not due to the presence of secondary structure, we examined the DNA-binding properties of RecA or SSB to a substrate that is lacking secondary structure. Figure 1 shows that RecA formed a complex with ssDNA that did not migrate beyond the origin of the gel (lane 6), whereas SSB produced a distinct complex with the same substrate that entered the gel (lane 7). Again, we observed that incubation of both RecA and SSB with the oligonucleotide substrate led to the formation of a single complex that had mobility similar to that of SSB−DNA complex (lane 8). The sizes of protein−DNA complexes were similar regardless of the order in which RecA and SSB were added to the reaction mixture. These results demonstrate that SSB converts heterogeneously sized protein−DNA complexes into a discrete protein−DNA complex.

The identity of a ternary complex of RecA−ssDNA−SSB was investigated by "supershift" assays. Thus, when anti-RecA antibody was added to the binding reaction, a further decrease in the mobility of protein−DNA complexes was observed (lane 6, Figure 2A). As expected, this effect was not evident with DNA alone or SSB−DNA complex. A parallel assay was performed to test the ability of anti-SSB antibody to retard the mobility of RecA−ssDNA−SSB complex. As shown in Figure 2B (lanes 6 and 7), anti-SSB antibody retarded the mobility of SSB−ssDNA−RecA complex, whereas control samples showed that SSB antibody failed to retard DNA. Together, these results suggest that 52-mer DNA support the simultaneous binding of both RecA and SSB. Importantly, however, these data indicate that SSB binding to the oligonucleotide containing stem loop failed to prevent the binding of RecA or vice versa.

Having established the presence of both RecA and SSB in the nucleoprotein filament, we wished to investigate whether this complex contains stoichiometric amounts of RecA and SSB. Gel filtration was used to separate unbound ^{35}S-labeled RecA and ^{35}S-labeled SSB from that bound to the labeled 52-mer DNA. Analyses of data revealed that only ^{35}S-labeled RecA was associated with the labeled 52-mer DNA (4 nucleotide residues/monomer). In controls, both ^{35}S-labeled RecA and ^{35}S-labeled SSB were incubated with M13 ssDNA and the nucleoprotein complexes were isolated by gel filtration. Consistent with previous reports (*16*, *33*), both ^{35}S-labeled RecA (3 nucleotide residues/monomer) and ^{35}S-labeled SSB (16 nucleotide residues/monomer) were associated with M13 ssDNA. One possible explanation for the lack of SSB in the nucleoprotein complex is that SSB dissociates from 52-mer DNA under conditions used for gel filtration. However, pair wise comparison of "supershift" experiments demonstrated the presence of both RecA and SSB in the nucleoprotein complex.

Binding of RecA and SSB to the Stem Loop Inhibits HaeIII Cleavage. It has been established that certain type II restriction endonucleases cleave ssDNA by virtue of secondary structure in the DNA (*40*). To further investigate the binding of RecA to the stem loop, an oligonucleotide sequence was designed such that when it folds into stem loop configuration, it generates a restriction site for *HaeIII*. We monitored the accessibility of such a site to *HaeIII* in the absence or presence of RecA or SSB. In control samples, digestion of 5′-labeled 52-mer DNA was performed under three different assay conditions. Deproteinized reaction products were separated by denaturing gel electrophoresis and visualized by autoradiography. When assayed by this system, control reactions showed efficient cleavage generating 20-mer DNA fragment corresponding to the 5′ end of the substrate (lanes 2−4, Figure 3A). We next asked whether incubation of labeled 52-mer DNA with RecA in reactions containing ATP provide protection from *HaeIII* cleavage. For comparison, identical reactions were performed in the presence of ATPγS. The gel image in Figure 3A shows that a 20-mer DNA product was generated only in reactions performed with RecA in the presence of ATP, but not with ATPγS (compare lanes 5−8 versus 9−12). The gel image in Figure 3A was quantified to assess the extent of cleavage. As shown in Figure 3B, in the presence of ATPγS, protection was effective, and after 10 min, >95% of the ^{32}P-labeled substrate was found to have participated in the binding reaction with RecA. On the other hand, incubations performed in the presence of ATP provided no measurable protection under identical conditions. The overall protection observed in the presence of ATPγS may reflect the binding of RecA to the stem loop. However, this pattern of inhibition is readily explained by the following. First, *HaeIII* is prevented from accessing the cleavage site embedded in the RecA−DNA complex. Second, RecA disrupts stem loop resulting in loss of cleavage. It is not clear which of these possibilities reflect the protection pattern observed with samples in the presence of RecA.

To extend the data presented in Figure 3, where RecA in the presence of ATP failed to protect stem loop from *HaeIII* cleavage, a complementary experiment was conducted to investigate whether SSB would facilitate RecA in conferring protection against *HaeIII* digestion. As shown in Figure 4,

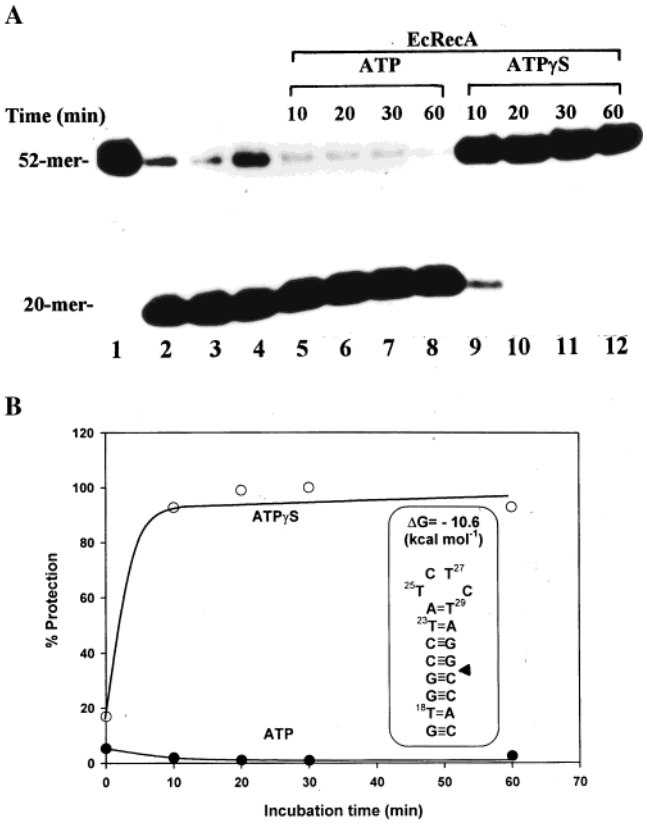

FIGURE 3: Kinetics of disruption of stem loop structure. (A) Protection of the *HaeIII* cleavage site following binding of RecA to the stem loop structure. Reactions were performed with 3 μM ^{32}P-labeled oligonucleotide ($\Delta G = -10.6$) in *HaeIII* (lane 2) or RecA (lanes 3−12) assay buffer containing 1 mM ATP (lanes 3 and 5−8) or 0.1 mM ATPγS (lanes 4 and 9−12) in the absence (lanes 2−4) or presence (lanes 5−12) of 1 μM RecA. Samples were incubated at 37 °C for 10 min (lanes 5 and 9), 20 min (lanes 6 and 10), 30 min (lanes 7 and 11) and 60 min (lanes 8 and 12). Subsequently, samples were incubated with (lanes 2−12) 10 units of *HaeIII* for 30 min at 37 °C (10 units of *HaeIII* was sufficient to cleave all of the substrate DNA in the reaction mixture within 5 min in the absence of RecA binding). Reaction was stopped by the addition of EDTA to a final concentration of 50 mM. Lane 1 depicts a control reaction lacking any added protein. Samples were separated on a 12% denaturing polyacrylamide gel and visualized by autoradiography as described in the Experimental procedures. The position of substrate (52-mer) and product (20-mer) is indicated on the left. (B) Quantitation of the extent of protection conferred by RecA in the presence ATP or ATPγS from *HaeIII* cleavage. The arrowhead in the inset indicates the site of *HaeIII* cleavage.

the stimulatory effect of SSB on RecA is evident when nucleoprotein filaments were assembled with the addition of substoichiometric concentrations of SSB followed by RecA or vice versa. Such an interaction between SSB and RecA in the presence of ATP argues that SSB helps RecA in conferring protection to stem loop.

To further characterize the binding specificity of RecA to the stem loop, competition experiments were performed. For these assays, 1 μM RecA was incubated with 3 μM 52-mer DNA ($\Delta G = -10.6$ kcal mol^{-1}) with RecA in the presence of 0.1 mM ATPγS for 10 min. RecA−DNA complexes were challenged with 10-fold molar excess of a series of unlabeled oligonucleotide substrates differing in the amount of secondary structure ($\Delta G = -5.1$ to -14.7 kcal mol^{-1}). Thirty minutes after the addition of competitor, *HaeIII* was added and the samples were incubated for 30 min at 37 °C. We reasoned that the competitor DNA would sequester RecA

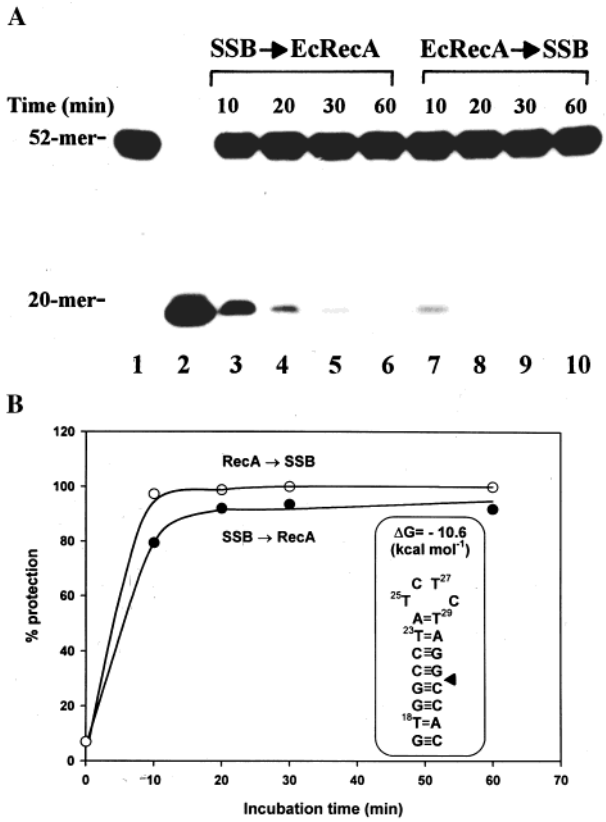

FIGURE 4: Kinetics of disruption of stem loop structure: effect of SSB. (A) SSB augments RecA in the presence of ATP in providing resistance to *HaeIII* cleavage. Reactions were performed in RecA assay buffer containing 3 μM ^{32}P-labeled oligonucleotide ($\Delta G = -10.6$), 1 mM ATP, 1 μM RecA, and 0.2 μM SSB. Samples were incubated at 37 °C for 10 min (lanes 3 and 7), 20 min (lanes 4 and 8), 30 min (lanes 5 and 9), and 60 min (lanes 6 and 10). Subsequently, samples were incubated with (lanes 2−10) 10 units of *HaeIII* for 30 min at 37 °C. Lane 1 represents a control reaction lacking any added protein. Reaction was stopped by the addition of EDTA to a final concentration of 50 mM. Samples were separated on a 12% polyacrylamide gel and visualized by autoradiography as described in the Experimental procedures. Arrows on the top of lanes indicate the order in which SSB (for 5 min) and RecA (for 10 min) were incubated with ssDNA. (B) Quantification of the extent of protection from *HaeIII* cleavage. The arrowhead in the inset indicates the site of *HaeIII* cleavage.

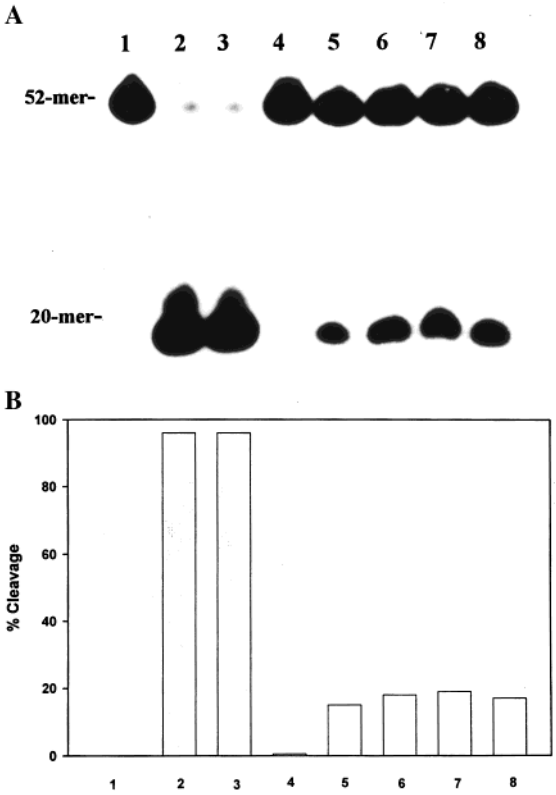

FIGURE 5: RecA bound to stem loop is resistant to higher amounts of competitor DNA containing different amounts of secondary structure. (A) Effect of heterologous ssDNA. Reactions were performed with 3 μM ^{32}P-labeled oligonucleotide ($\Delta G = -10.7$), 1 μM RecA and 0.1 mM ATPγS as described in the legend to Figure 3. Subsequently, samples (lanes 2−8) were incubated with 30 μM unlabeled ssDNA for 30 min and then treated with 10 units of *HaeIII* for an additional 30 min at 37 °C. Lane 1 depicts a control reaction lacking any added protein or competitor ssDNA; lane 2, *HaeIII* digestion carried out in the absence of RecA in an assay buffer as specified by the manufacturer; lane 3, RecA assay buffer; lane 4, complete reaction in the absence of added unlabeled competitor ssDNA. The remaining lanes contained the indicated competitor DNA as follows. Lane 5, $\Delta G = -14.7$; lane 6, $\Delta G = -7.4$; lane 7, $\Delta G = -6.6$; lane 8, $\Delta G = -5.1$. Samples were separated on a 12% polyacrylamide gel and visualized by autoradiography as described in the Experimental Procedures. The position of substrate (52-mer) and product (20-mer) is indicated on the left. (**B**) Quantification of the extent of cleavage in the presence of different competitor ssDNA substrates. The percentage of protection is plotted against the type of competitor ssDNA. Arabic numbers on the *x*-axis correspond to the respective lanes of Figure 5A.

from the ^{32}P-labeled 52-mer DNA and thus might provide a quantitative view of the stability of RecA−DNA complex. Under these conditions, only a fraction of DNA−RecA complexes was dissociated as revealed by the accumulation of a small amount of 20-mer product (Figure 5). We note that competition experiments compare binding affinities for different DNA substrates under solution conditions and are not sensitive to differences in the stability of protein−DNA complex during processing of the samples for electrophoresis. Significantly, all of the oligonucleotide substrates competed with similar efficiency despite possessing varying amounts of secondary structure.

In light of the above observations, it was of interest to explore whether increasing concentrations of ssDNA would compete with RecA that is bound to the stem loop. To test this possibility, complexes of ^{32}P-labeled DNA ($\Delta G = -10.6$ kcal mol^{-1}) and RecA were formed in the presence of ATPγS. After 30 min incubation, increasing amounts of unlabeled 52-mer DNA ($\Delta G = -10.6$ kcal mol^{-1}) was added to the reaction mixture with thorough mixing. Subsequently, reaction mixtures were allowed to reach binding equilibrium over a period of 30 min. To monitor displacement of RecA from the ^{32}P-labeled ssDNA containing stem loop, we treated samples with concentrations of *HaeIII* sufficient to cleave all of the added substrate. Interestingly, as seen in Figure 6, the magnitude of competition with increasing concentrations of unlabeled DNA was similar, suggesting that RecA binds the stem loop in a stable manner.

Binding of RecA to the Stem Loop Provoke Thymine Residues To React with KMnO$_4$. While DNA-binding behavior and competitor sensitivities provide indirect evidence for the specific binding of RecA and SSB to the stem loop, direct evidence for the disruption of stem loop can be pursued by more sensitive assays. One of these is the enhanced sensitivity of thymine (T) residues in the stem loop to reaction with $KMnO_4$ (*41*). The chemical mechanism of the

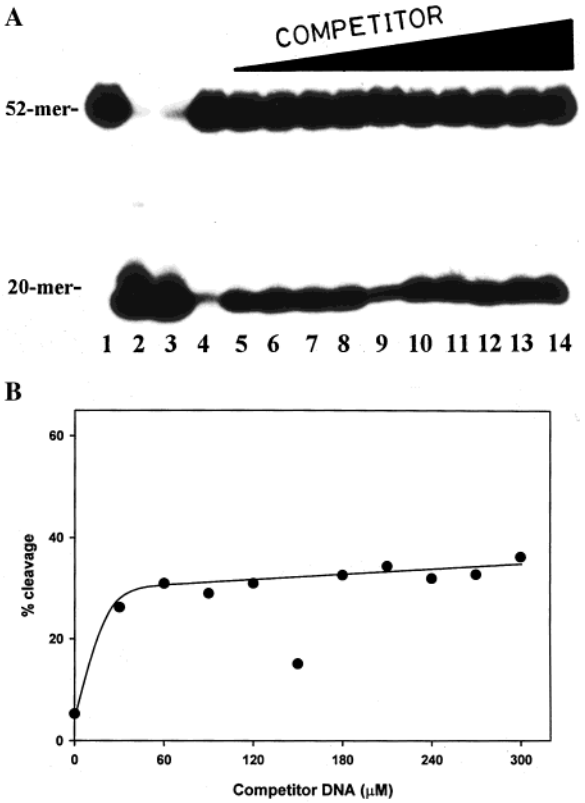

FIGURE 6: RecA bound to stem loop is resistant to dissociation by increasing amounts of competitor ssDNA. (A) Competition with homologous ssDNA. Reactions were performed in the presence of 0.1 mM ATPγS as described in the legend to Figure 3. Nucleoprotein filaments of RecA−ssDNA were incubated with increasing amounts of unlabeled oligonucleotide ($\Delta G = -10.6$) for an additional 30 min. The relative mass of unlabeled competitor DNA was (from lane 5) 10, 20, 30, 40, 50, 60, 70, 80, 90, and 100-fold excess. Subsequently, samples (lanes 2−14) were treated with 10 units of *HaeIII* for 30 min at 37 °C. Lane 1 depicts a control reaction lacking any added protein or competitor ssDNA; lane 2, digestion carried out in *HaeIII* assay buffer plus contained 100-fold excess of competitor; lane 3, RecA assay buffer plus 100-fold excess of competitor DNA. Samples were separated on a 12% denaturing polyacrylamide gel and visualized by autoradiography as described in the Experimental Procedures. The position of substrate (52-mer) and product (20-mer) is indicated on the left. (B) Quantitation of the extent of cleavage in the presence of excess of homologous competitor ssDNA. The percentage of protection is plotted against concentration of added unlabeled competitor ssDNA.

reaction involves attack on the π orbital of C5═C6 bond of T residue by $KMnO_4$ thereby converting to *cis*-thymine glycol. Base-paired T residue is insensitive to reaction with $KMnO_4$. The binding of RecA or SSB, or both proteins together, presumably would melt stem loop and, consequently, the T residues in the stem might become accessible to oxidation by $KMnO_4$. This approach is likely to provide direct evidence as to the kinetics of disruption of stem loop in real time.

We subjected RecA to quantitative kinetic analysis of disruption of stem loop using a collection of ssDNA substrates that contain varied amounts of secondary structure. Kinetics of disruption of stem loop was monitored by the sensitivity of T residues to reaction with $KMnO_4$ using 52-mer DNA ($\Delta G = -7.4$ kcal mol^{-1}). After cleavage of modified bases with piperidine, DNA fragments were separated on 12% polyacrylamide gels in the presence of 8 M urea. In the absence of RecA or SSB, T23 and T29 residues displayed no sensitivity to $KMnO_4$ modification over the background levels (Figure 7A). In the presence of ATPγS, however, RecA rendered T23 and T29 residues sensitive to $KMnO_4$ modification in a time-dependent manner (as judged by the fraction of the substrate unfolded in relation to the control lane). To test the requirement of ATP hydrolysis for the disruption of stem loop, reactions were performed in the presence of 1 mM ATP. However, with ATP as the nucleotide cofactor RecA failed to stimulate both T29 and T23 residues to reaction with $KMnO_4$ over the background levels. To validate the $KMnO_4$ probing assay, identical reactions were performed with SSB alone or both SSB and RecA. In these reactions, the sensitivity of T23 residue paralleled those reactions performed in the presence of ATPγS (lanes SB and SR, Figure 7A).

To reinforce the $KMnO_4$ modification assay, the amplitude of relevant bands corresponding to T residues in the stem loop structure was quantified by scanning the autoradiogram. The extent of modification was plotted (in arbitrary units) versus time of incubation (Figure 7B). In the presence of ATPγS, but not ATP, the sensitivity of T23 and T29 residues in the stem to reaction with $KMnO_4$ increased during the period of incubation. The band intensity of T23 residue extrapolated through the origin and increased linearly under these conditions, while the intensity of T29 increased with reaction time and found to plateau in <10 min. Intriguingly, in the presence of ATPγS, but not ATP, RecA rendered the T25 and T27 residues in the loop hypersensitive to reaction with $KMnO_4$, suggesting that the residues encompassing the loop might flip out to become readily accessible to modification. These results indicate that four nucleotide residues in the loop is sufficient for stable binding of RecA, and consistent with the site-size reported previously, argue that RecA monomer is the minimum binding unit (see below).

RecA Initiates Disruption of Stem Loop at the Loop Region. To determine the path of disruption of stem loop by RecA, we utilized a 52-mer DNA ($\Delta G = -10.6$ kcal mol^{-1}) with T residues situated at the proximal and distal ends of the stem to monitor their sensitivity to reaction with $KMnO_4$. Also, we wished to confirm the minimum binding unit of RecA. Visual inspection of a representative gel image shows that a higher amount of secondary structure significantly influenced the modification profiles of all three T residues in the stem (Figure 8A). We note that the band intensity of T29 residue is somewhat high in control reactions. One possible reason for the high background value might be due to the fact that the A:T base pair bordering the loop breathes or flips out of the stem, which is consistent with the behavior of DNA in solution (*42*). In the presence of ATPγS, RecA rendered both T29 and T23 residues hypersensitive (by 2−3-fold) and reached a plateau in <5 min. Significantly, the band intensity of T18 residue, which is 7 bp down in the stem, increased linearly and extrapolated through the origin (Figure 8B). Unlike ATPγS, ATP failed to support RecA in enhancing the sensitivity of all three T residues in the stem to reaction with $KMnO_4$. In reactions performed with SSB or both RecA and SSB, the extent of modification of T residues in the stem (lanes SB, and SR, Figure 8A) was similar to that induced by RecA in the presence of ATPγS. Importantly, RecA rendered T residues in the loop hypersensitive to reaction with $KMnO_4$, thereby favoring the notion that RecA monomer is the minimum

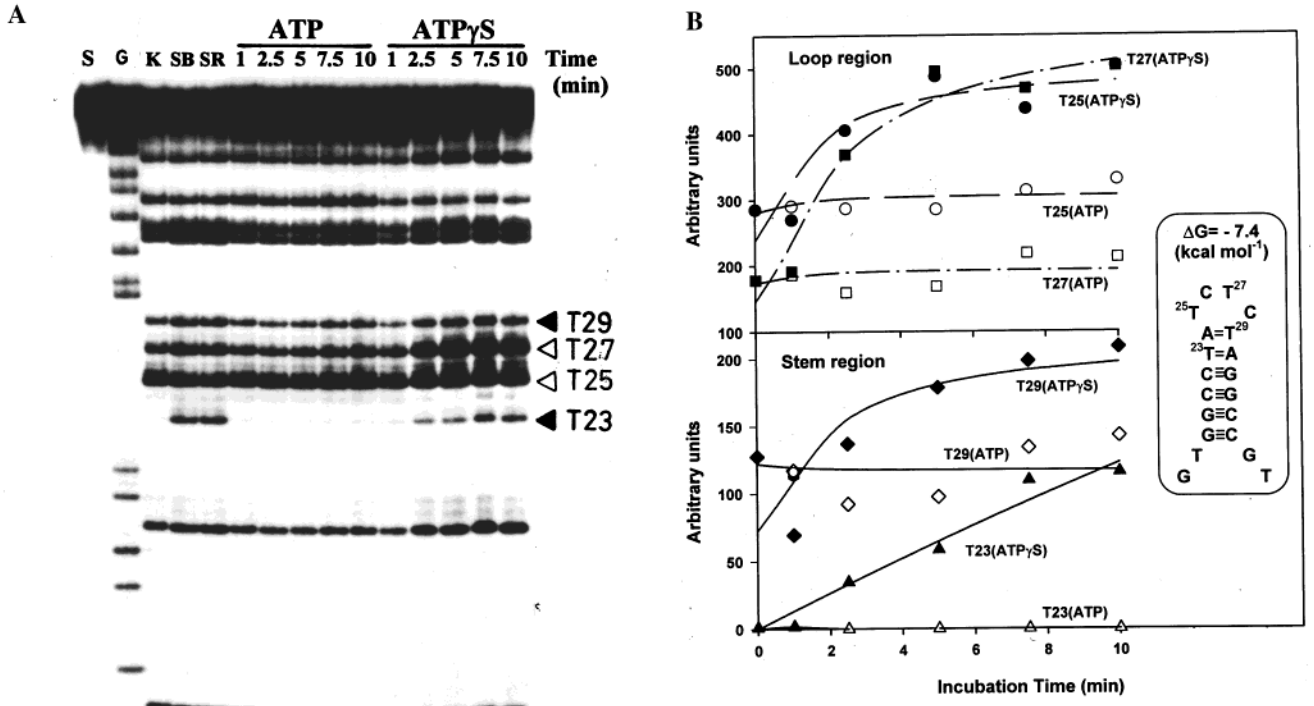

FIGURE 7: RecA enhances the reactivity of thymine residues in the stem loop with potassium permanganate. (A) Chemical reactivity of T residues in the stem loop in the presence RecA and ATP or ATPγS. Reaction mixtures contained 3 μM ^{32}P-labeled oligonucleotide ($\Delta G = -7.4$), 1 μM RecA, 1 mM ATP, or 0.1 mM ATPγS. Lanes from left to right: S, substrate; G, Maxam−Gilbert G sequencing ladder; K, control reaction performed with $KMnO_4$ in the absence of added proteins; SB, control reaction carried out with 0.2 μM SSB for 1 min followed by treatment with $KMnO_4$; SR, control reaction performed with 1 μM RecA and 0.2 μM SSB for 1 min followed by treatment with $KMnO_4$. The remaining samples were incubated with RecA for the time periods as indicated above each lane. Samples were treated with $KMnO_4$ and analyzed as described in the Experimental Procedures. Open and closed arrowheads indicate the locations of T residues in the stem and loop, respectively. Numbers refer to positions of T residues in the oligonucleotide. (B) The reactivity profiles of relevant T residues with $KMnO_4$ in the loop and stem regions as determined by scanning the autoradiogram shown in panel A with a UVItech gel documentation system using UVIBAND 97.04 software. The extent of modification (arbitrary units) of the specified T residues is plotted versus the time of incubation with RecA in the presence of ATP or ATPγS.

binding unit. The pattern of modification of T residues in the flanking sequences by $KMnO_4$ is unchanged in the presence or absence of RecA or SSB. We are unable to specify the molecular event responsible for RecA-induced hypersensitivity of T residues in the loop but not in the flanking sequences. In this regard, we note that Rad51 protein caused enhanced fluorescence of 2-aminopurine in the context of duplex DNA (*43*). Together, these results suggest that RecA initiates disruption of stem at the loop region and then propagated down the stem. Similar results were obtained with oligonucleotides containing $\Delta G = -7.4$ and -14.7 kcal mol^{-1} (data not shown).

Polarity of RecA Binding on ssDNA Is Uninterrupted in the Presence of SSB. The data presented above indicate that contiguous binding of RecA is halted at the proximal end of the stem. Subsequent binding and elongation of the RecA filament down the stem requires ATPγS. We then examined the kinetics of disruption of stem loop in reactions containing RecA and SSB. For direct comparison, reactions were performed with the 52-mer DNA containing $\Delta G = -10.6$ kcal mol^{-1}. Visual inspection of the gel image versus time of incubation shows that disruption of stem loop as noted by the band intensities of T18, T23, and T29 residues situated in the stem was robust (Figure 9A). The kinetics of modification of relevant T residues suggest that disruption of stem loop was efficient and largely completed in <2 min (Figure 9B). That the rapid time course of disruption of T18 residue in the presence of SSB and ATP is to be compared with the linear time course in the presence of ATPγS (Figure 8B). Significantly, T residues in the loop, but not in the flanking sequences, displayed higher sensitivity to reaction with $KMnO_4$. This is strikingly similar to that obtained with RecA and ATPγS, thereby indicating binding of both RecA and SSB to the stem loop.

Stability of RecA−DNA Complexes. To further understand the relative affinity of RecA to stem loop, we examined the stability of RecA−DNA complexes. More specifically, we wished to investigate whether RecA−DNA complexes formed with stem loop would be stable at 4 °C, a condition that induces the formation and stabilization of secondary structure. Nucleoprotein filaments of RecA−DNA ($\Delta G = -7.4$ kcal mol^{-1}) were formed in the presence of ATPγS at 37 °C. One set of samples was incubated at 37 °C and a second set of samples at 4 °C. After the indicated time

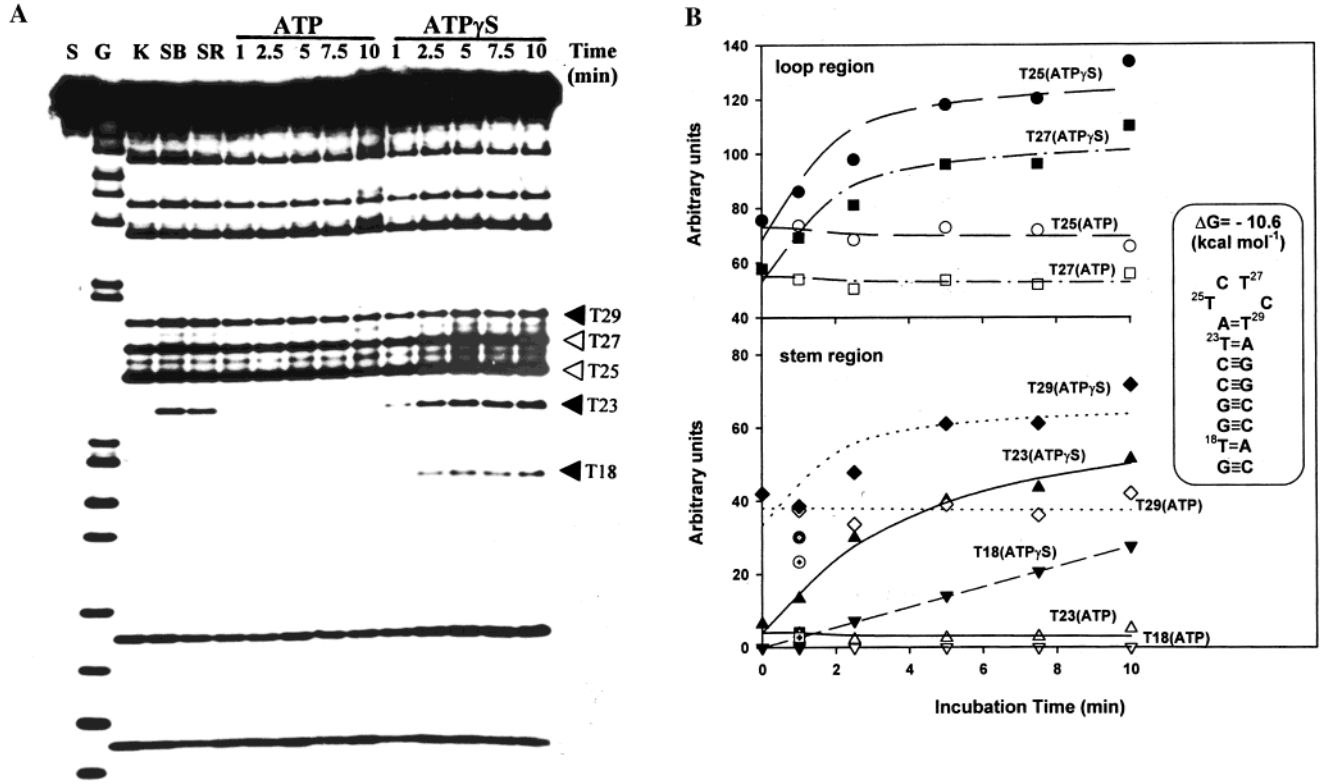

FIGURE 8: RecA preferentially enhances the reactivity of T residues in the distal end of the stem with $KMnO_4$. (A) Kinetics of reactivity of T residues with $KMnO_4$ reveals the path of disruption of stem loop by RecA. Reactions were performed as described in the legend to Figure 7A, except that the [^{32}P]oligonucleotide used to form nucleoprotein filaments with RecA, SSB, or with both proteins, contained a ΔG of -10.6. Lanes from left to right: S, substrate alone; G, Maxam−Gilbert G sequencing ladder; K, control reaction performed with $KMnO_4$ in the absence of added proteins; SB, control reaction carried out with 0.2 μM SSB for 1 min followed by treatment with $KMnO_4$; SR, control reaction performed with 1 μM RecA and 0.2 μM SSB for 1 min followed by treatment with $KMnO_4$. The remaining samples were incubated with RecA for the time periods as indicated above each lane. Samples were incubated with $KMnO_4$ and analyzed as described in the Experimental Procedures. Open and closed arrowheads indicate the locations of T residues in the stem and loop, respectively. Numbers refer to positions of T residues in the oligonucleotide. (B) Quantitation of preferential reactivity of T residues in the stem loop structure in the presence of RecA as determined by scanning the autoradiogram shown in panel A with a UVItech gel documentation system using UVIBAND 97.04 software. The extent of modification (arbitrary units) of specified T residues is plotted versus the time of incubation with RecA in the presence of ATP or ATPγS.

intervals, samples were subjected to $KMnO_4$ modification assay. Reactions were terminated, and samples were deproteinized as described in the Experimental Procedures. Deproteinized products were separated by denaturing gel electrophoresis and visualized by autoradiography. To assay the induction of secondary structure, we monitored the sensitivity of T23 residue situated in the distal portion of stem to reaction with $KMnO_4$. The data in Figure 10 show that the band intensity of T23 residue was not significantly changed between samples incubated at 37 and 4 °C, suggesting that ssDNA substrate failed to fold into a stem loop. These results imply that RecA−DNA complex is resistant to conditions that induce the formation and stabilization of secondary structure.

DISCUSSION

In the present study, two sets of experiments were carried out. In the first series, we characterized the influence of secondary structure on the DNA-binding and ATPase activities of RecA. The data in Table 2 show that the rate of ATP hydrolysis decreased with increased amount of secondary structure. The most notable difference between RecA and SSB is in their ability to interact with substrates containing stem loop structures. In contrast to RecA, binding of SSB to these substrates is rapid and efficient. The extent of formation of RecA−DNA complexes was dependent on the amount of secondary structure. Electrophoretic mobility shift and "supershift" assays show that SSB forms a discrete complex with 52-mer DNA, regardless of the presence or absence of secondary structure. This observation is consistent with earlier studies showing that a SSB tetramer can bind to ssDNA fragments as short as 30−36 nucleotide residues (*44*). When similar assays were performed with RecA, two distinctly different complexes were generated depending on the nature of ssDNA substrate. RecA protein generated a distinct complex with ssDNA lacking secondary structure. By contrast, with a series of oligonucleotides harboring stem loop, RecA displayed a smear of labeled DNA with one major band that failed to enter the gel. Intriguingly, incubation of the same substrate with RecA and SSB produced a discrete complex. The notion that both SSB and RecA coexist in this complex was ascertained by "supershift" experiments. The formation of nucleoprotein complex of SSB−ssDNA−RecA suggests that SSB and RecA form an integrated complex in which both are in direct contact with ssDNA. However, others have reported that RecA and SSB are mutually exclusive for ssDNA binding, and this exclusive occupancy may define whether RecA manifests maximal ATPase, homologous pairing and strand exchange activities (*23*, *24*).

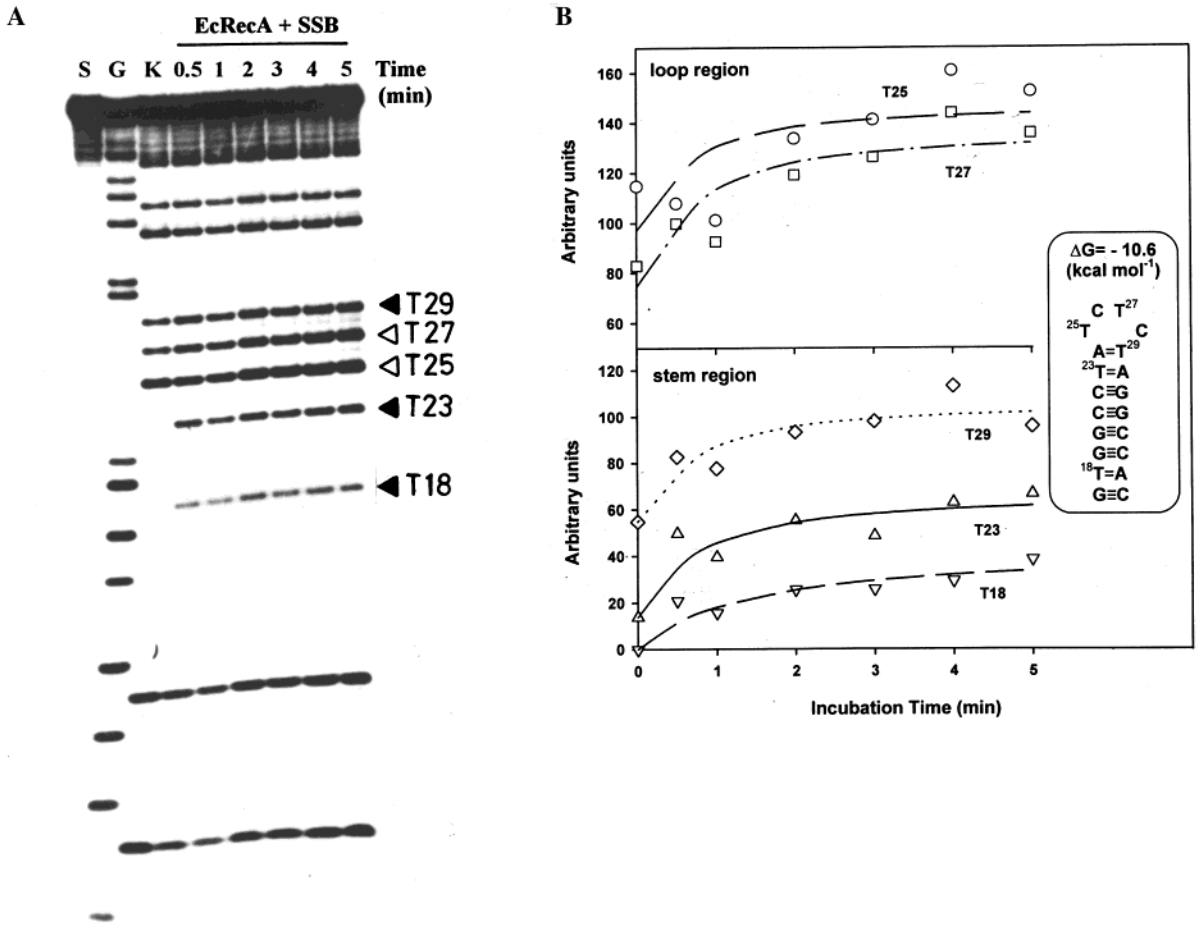

FIGURE 9: SSB facilitates contiguous binding of RecA. (A) Kinetics of disruption of stem loop by RecA and SSB. Reactions were performed as described in the legend to Figure 7A with the same [^{32}P]oligonucleotide ($\Delta G = -10.6$) and RecA and SSB in the presence of 1 mM ATP for the indicated time intervals. Lanes from left to right: S, substrate alone; G, Maxam−Gilbert G sequencing ladder; K, control reaction performed with $KMnO_4$ in the absence of SSB and RecA. The remaining samples were incubated with RecA and SSB for the time intervals as indicated above each lane. Samples were incubated with $KMnO_4$ and analyzed as described in the Experimental procedures. Open and closed arrowheads indicate the locations of T residues in the stem and loop, respectively. Numbers refer to positions of T residues in the oligonucleotide. (B) Quantitation of preferential reactivity of T residues in the stem loop structure in the presence of SSB and RecA as determined by scanning the autoradiogram shown in panel A with a UVItech gel documentation system using UVIBAND 97.04 software. The extent of modification (arbitrary units) of specified T residues is plotted versus the time of incubation with RecA and SSB in the presence of ATP.

Our comprehensive analysis of the influence of secondary structure on the DNA-binding parameters of SSB and RecA using a number of different approaches has led to several new insights. The relationship that we have explored is significant in that it firmly establishes the mechanism by which SSB facilitates the reactions promoted by RecA. Although extensive work has been carried out to elucidate the role of SSB in all of the reactions performed by RecA, a caveat of these studies is the use of large circular ssDNA substrates that do not permit clear resolution of mechanistic issues. The results obtained thus far support a model in which SSB plays an important role in the assembly of RecA nucleoprotein filament. The effect of SSB is interpreted by the presumption that it melts out secondary structure in ssDNA, thereby facilitating the formation of a helical nucleoprotein filament of RecA. In this study, we used oligonucleotides to focus on short-range structural barriers to RecA polymerization. This would exclude constraints associated with the topological barriers imposed by long circular ssDNA and interpretation of data from complex indirect assays.

Although SSB is crucial for the display of maximal activity of RecA-mediated reactions, a number of other DNA-binding proteins modulate the assembly and disassembly of nucleoprotein filaments of RecA−ssDNA (reviewed in ref *45*). In *E. coli*, the most prominent components are RecF, RecO, and RecR proteins. Several lines of evidence indicate that RecF, RecO, and RecR proteins function as a part of nucleoprotein complex. For example, RecO and RecR proteins stimulate binding of RecA onto ssDNA complexed with SSB (*46*, *47*). Consequently, the resulting nucleoprotein filament containing RecA, RecO, RecR, and SSB displayed about 70% activity in DNA−DNA pairing and strand exchange reactions (*46*). RecOR proteins apparently stimulate the rate of formation of joint molecules with no effect on the rate of strand exchange. Consistent with these observations, it has been demonstrated that RecO physically interacts with both SSB and RecR proteins. Further studies have shown that RecO and RecR proteins block end-dependent disassembly of RecA from linear ssDNA (*48*). How secondary structure modulates the functions(s) of RecFOR proteins individually, and together with SSB and RecA, remains to be elucidated.

Specific protein−protein interaction has also been detected between RecF and RecR proteins. However, biochemical studies have not yet demonstrated positive effect(s) of RecF

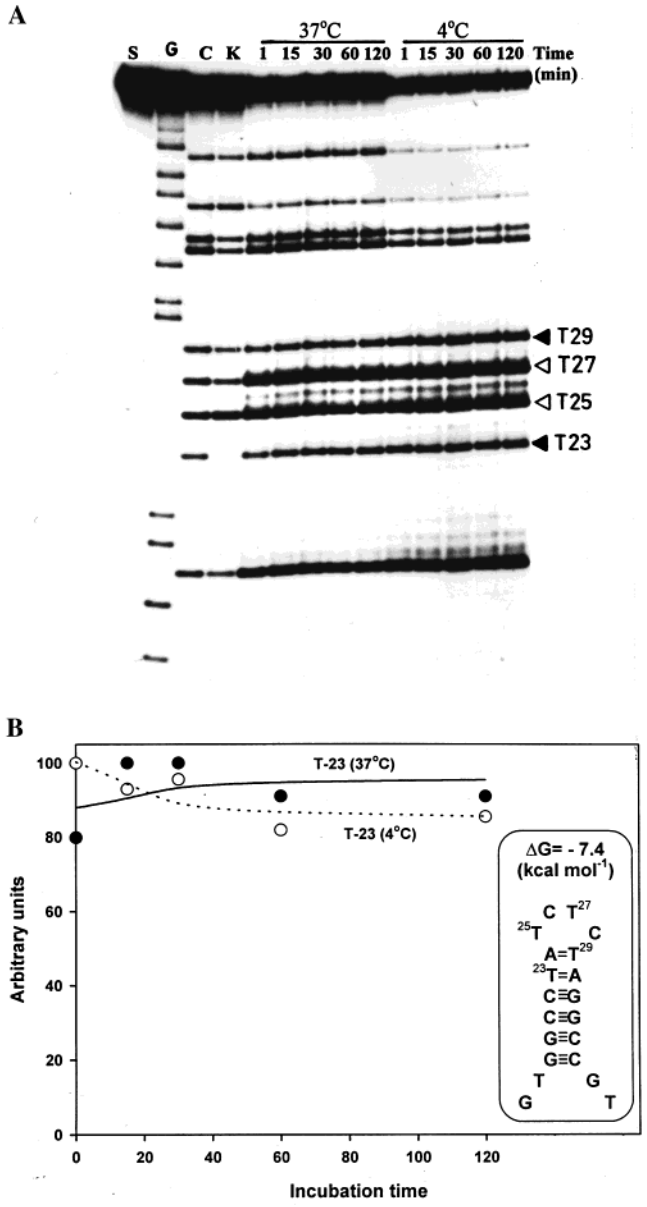

FIGURE 10: Nucleoprotein filaments of RecA−ssDNA are stable at 4 °C. (A) Absence of reformation of stem loop structure. RecA−ssDNA complexes were formed by incubating 3 μM ^{32}P-labeled 52-mer DNA ($\Delta G = -7.4$), 1 mM RecA, in the presence of 0.1 mM ATPγS as described in the Experimental procedures. Subsequently, One set of samples was incubated at 37 °C and a second set at 4 °C for time periods as indicated above each lane. Samples were treated with $KMnO_4$ and analyzed as described in the Experimental procedures. Lanes from left to right: S, substrate; G, Maxam−Gilbert G sequencing ladder; C, control reaction performed in the presence of 0.2 μM SSB and then reacted with $KMnO_4$; K, control reaction carried out with $KMnO_4$ in the absence of added proteins. Open and closed arrowheads indicate the locations of T residues in the stem and loop, respectively. Numbers refer to positions of T residues in the oligonucleotide. (B) The reactivity profiles of T23 residues with $KMnO_4$ as determined by scanning the autoradiogram shown in panel A with a UVItech gel documentation system using UVIBAND 97.04 software. The extent of modification (arbitrary units) of T23 residue is plotted versus the time of incubation at the indicated temperatures.

protein on the activity of RecOR in the assembly of RecA nucleoprotein filaments and prevent end-dependent disassembly of those filaments. At high concentrations, RecF inhibits binding of RecA protein onto ssDNA, thereby prohibiting the three-strand exchange reaction promoted by RecA. This inhibition is not observed in the presence of RecO and RecR proteins. It appears, however, that RecFR proteins participate in recombinational repair of DNA wherein RecFR proteins, acting together, bind randomly to duplex DNA and restrict the continuous assembly of RecA nucleoprotein filament into the adjoining duplex regions from ssDNA gap (*49*). After nucleation of RecA on ssDNA, elongation of the RecA filament is unidirectional and proceeds in a 5′ to 3′ direction to form a contiguous helical nucleoprotein filament (*50*−*52*). This path appears to determine the directionality of strand exchange with respect to the initiating ssDNA. Like the assembly process, the major pathway of disassembly of nucleoprotein filament of RecA−ssDNA is also unidirectional (*52*). On linear ssDNA nucleation presumably occurs at multiple random sites and proceeds toward the 3′-end (*52*, *53*). Since the nucleoprotein filament serves as an intermediate in all of the reactions promoted by RecA, studies on the assembly of RecA filament have played a key role in our understanding of the initiation of recombination and repair processes (for reviews, see refs *18*−*20*). However, differential effects imposed by structural barriers to the progression of RecA filament assembly, and how SSB helps to relieve the barrier, have not been studied in sufficient detail. How do structural barriers such as stem loop structures affect unidirectional elongation of RecA nucleoprotein filament? Does the stem loop cause abrupt termination or pausing of filament elongation? What is the path of disruption of stem-loop structure: from the proximal or distal end of the stem? What is the minimum binding unit of RecA?

To gain insights into the issues raised above, we performed $KMnO_4$ modification reactions, which have provided information about the manner by which RecA and SSB cause disruption of stem loop. This sensitive method facilitated direct measurement of kinetics of disruption of stem loop, which might have been undetectable by conventional methods. Although both RecA and SSB promote disruption of stem loop, there are notable differences in the kinetics and the mechanism of disruption. RecA-stimulated reactivity of T residues with $KMnO_4$ can be divided into three categories: substantial hypersensitivity at the loop, large enhancement at the distal end of the stem, and slow but linear increase at the proximal end. The kinetics of modification of T residues at the proximal end of the stem is rather slow. By contrast, modification of T residues at the distal end of the stem is much faster. Consequently, the relative differences in the band intensity of T residues at the proximal versus the distal end argue that disruption of stem loop by RecA begin at the loop region and elongation of the RecA filament down the stem causes its disruption.

The thermodynamic explanation for stalling RecA polymerization at the proximal end of the stem remains outstanding. ATP hydrolysis is not required for contiguous binding of RecA on to ssDNA (*18*−*20*). Paradoxically, ATP hydrolysis failed to elongate RecA filament across stem loop in ssDNA. Binding of RecA to the loop arises naturally because it displays high affinity to ssDNA. Significantly, a binding site size of four nucleotide residues in the loop is sufficient for RecA to display hypersensitivity of T residues. Although the mechanism is unknown, the modification profiles of T residues postulate alterations in the orientation of bases. Consistent with these observations, others have

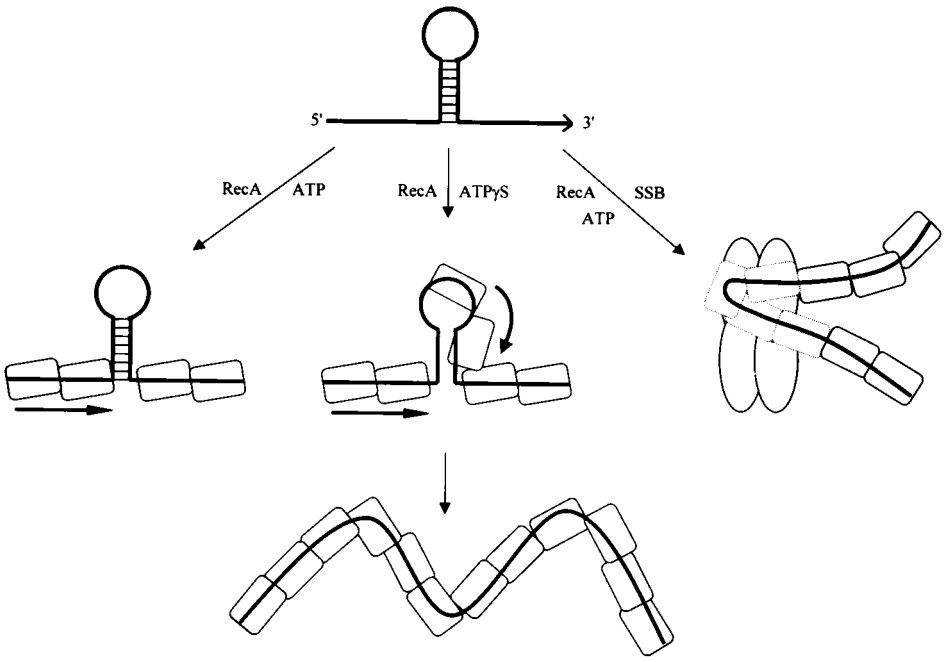

FIGURE 11: Model for disruption of stem loop structure by RecA and SSB. In the model, rectangles (continuous as well as dashed) represent RecA monomers and ovals denote monomers of SSB. In the presence of ATP (left), RecA binds mainly to the flanking nucleotide sequences of the stem loop. In the presence of ATPγS (center), RecA binds to the flanking sequences and at the loop region. The elongation of the RecA filament down the stem disrupts the stem and generates a helical nucleoprotein filament. In the right view, binding of SSB to the bases (ref *67*) and RecA to the phosphate backbone (ref *36*) results in the formation of a nucleoprotein filament comprised of RecA−ssDNA−SSB. Block arrows denote the polarity of polymerization of RecA on ssDNA containing stem loop (see Discussion for further details).

noted that RecA and Rad51 proteins perturb the orientation of bases upon their interaction with DNA (*43*, *54*, *55*).

Together with previous studies (*16*, *21*−*24*), our data suggest the following model (Figure 11). First, in the presence of ATPγS, nucleation of a RecA monomer at the loop initiates cooperative binding down the stem resulting in concomitant disruption of the stem loop structure. Second, in the presence of ATP, elongation of RecA filament is halted at the proximal end of the stem. Third, under physiological conditions, by melting secondary structure SSB ensures the directionality of RecA polymerization. These results implicate a novel role for SSB in the formation of an active nucleoprotein filament of RecA across structural barriers in ssDNA. Perhaps the more interesting inference is that RecA monomer appears to be the minimum binding unit.

What is the physiological significance of the in vitro function of SSB to the actual role of *ssb* gene product in the cellular context? Detailed genetic analyses of *ssb* mutants suggest specific role(s) for SSB in the pathway to homologous recombination and repair (*1*, *2*). Cells bearing *ssb-1* mutation (His55 to Tyr) reduce the frequency of conjugational recombination and P1 transduction (*2*, *4*). The *ssb-3* mutation (Gly15 to Asp) renders cells extremely UV sensitive and displays a 75% reduction in the frequency of conjugational recombination as measured by Hfr mating (*56*). In this regard, the data presented here suggest that one role of SSB is to facilitate contiguous binding of RecA across structural barriers in vivo to generate an active nucleoprotein filament.

The importance of stem loop structures has recently been highlighted by the discovery that human triplet expansion diseases and genetic instability arise, at least in part, from improper secondary structure (reviewed in ref *3*). Recent studies in model organisms have established that trinucleotide repeats associated with hereditary diseases form secondary structures in vivo. In the cases of *Saccharomyces cerevisiae* and *E. coli*, plasmids harboring sequences capable of folding into a triplet configuration enable the plasmids to delete large portions of DNA in a length-dependent manner (*58*−*60*). Work in vivo implies that trinucleotide expansions can occur during DNA replication and recombination processes (*61*). One possible adverse effect of stem loop structures emerges perhaps from their ability to interfere with the normal function of cellular machinery. For example, polymerase pausing or halting has been observed at triplet repeats (*61*). Genetic studies have shown that mismatches incorporated into stem loop structures were inefficiently repaired during meiotic recombination (*62*, *63*). Indeed, recent studies have shown that secondary structure inhibits flap processing of CAG, CGG, or CTG repeats by FEN-1 endonuclease leading to expansions in a site-specific manner (*64*). Consistent with these findings, yeast cells bearing *rad27*Δ mutation, which are deficient in 5′ to 3′ flap endonuclease (a homologue of FEN-1), display increased frequency of insertion events at many a repeat sequences throughout the genome (*65*, *66*). Our observation on RecA is congruent with those proteins that are involved in DNA repair and replication and also fit into the general framework of processes that require disruption of stem loop structures. In this scenario, RecA and SSB proteins are likely to provide useful paradigms for elucidating the role of secondary structure in many aspects of DNA metabolism.

ACKNOWLEDGMENT

We thank Mr. N. Guhan for his assistance in the preparation of Figure 11 and members for this laboratory for constructive suggestions.

REFERENCES

1. Lohman, T. M., and Ferrari, M. E. (1994) *Annu. Rev. Biochem. 63*, 527−570.
2. Meyer, R. R., and Laine, P. S. (1990) *Microbiol. Rev. 54*, 342−380.
3. McMurray, C. T. (1999) *Proc. Natl. Acad. Sci. U.S.A. 96*, 1823−1825.
4. Glassberg, J., Meyer, R. R., and Kornberg, A. (1979) *J. Bacteriol. 140*, 14−19.
5. Sigal, N., Delius, H., Kornberg, T., Gefter, M. L., and Alberts, B. (1972) *Proc. Natl. Acad. Sci. U.S.A. 69*, 3537−3541.
6. Baluch, J., Chase, J., and Sussman, R. (1980) *J. Bacteriol. 144*, 489−498.
7. Molineux, I. J., Friedman, S., and Gefter, M. L. (1974) *J. Biol. Chem. 249*, 6090−6098.
8. Weiner, J. H., Bertsch, L. L., and Kornberg, A. (1975) *J. Biol. Chem. 250*, 1972−1980.
9. Chase, J. W., L'Italian, J. J., Murphy, J. B., Spicer, E. K., and Williams, K. R. (1984) *J. Biol. Chem 259*, 805−814.
10. Lohman, T. M., and Overman, L. B. (1985) *J. Biol. Chem. 260*, 3594−3603.
11. Bujalowski, W., Overman, L. B., and Lohman, T. M. (1988) *J. Biol. Chem. 263*, 4629−4640.
12. Bujalowski, W., and Lohman, T. M., (1986) *Biochemistry 25*, 7799−7802.
13. Bujalowski, W., and Lohman, T. M., (1989) *J. Mol. Biol. 207*, 269−288.
14. Bujalowski, W., and Lohman, T. M., (1989) *J. Mol. Biol. 217*, 63−74.
15. Griffith, J. D., Harris, L. D., and Register, J., III (1984) *Cold Spring Harbor Symp. Quant. Biol. 49*, 553−559.
16. Muniyappa, K., Williams, K. R., Chase, J., and Radding, C. M. (1990) *Nucleic Acids Res. 18*, 3967−3973.
17. Wold, M. S. (1997) *Annu. Rev. Biochem. 66*, 61−92.
18. Kowalczykowski, S. C., Dixon, D. A., Eggleston, A. K., Lauder, S. D., and Rehrauer, W. M. (1994) *Microbiol. Rev. 58*, 401−465.
19. Rocca, A. I., and Cox, M. M. (1997) *Prog. Nucleic Acids Res. Mol. Biol. 56*, 129−223.
20. Kuzminov, A. (1999) *Microbiol. Mol. Biol. Rev. 63*, 751−813.
21. Morrical, S. W., and Cox, M. M. (1990) *Biochemistry 29*, 837−843.
22. Muniyappa, K., Shaner, S. L., Tsang, S. S., and Radding, C. M. (1984) *Proc. Natl. Acad. Sci. U.S.A. 81*, 2757−2761.
23. Kowalczykowski, S. C., Clow, J. C., Somani, R., and Varghese, A. (1987) *J. Mol. Biol. 193*, 81−95.
24. Kowalczykowski, S. C., and Krupp, R. A. (1987) *J. Mol. Biol. 193*, 97−113.
25. Chiu, S. K., Wong, B. C., and Chow, S. A. (1990) *J. Biol. Chem. 265*, 21262−21268.
26. Lavery, P. E., and Kowalczykowski, S. C. (1992) *J. Biol. Chem. 267*, 9315−9320.
27. Mazin, A. V., and Kowalczykowski, S. C. (1998) *EMBO J. 17*, 1161−1168.
28. Xodo, L E., Manzini, G., Quadrifoglio, F., van der Marel, G. A., and van Boom, J. H. (1991) *Nucleic Acids Res. 19*, 1505−1511.
29. Sambrook, J., Fritsch, E. F., and Maniatis, T. (1989) *Molecular Cloning: A laboratory Manual*, 2nd ed., Cold Spring Harbor Laboratory Press, Plainview, New York.
30. Cunningham, R. P., DasGupta, C., Shibata, T., and Radding, C. M. (1980) *Cell 20*, 223−235.
31. Griffith, J., and Shores, G. C. (1985) *Biochemistry 24*, 158−162.
32. Lohman, T. M., Green, J. M., and Beyer, R. S. (1986) *Biochemistry 25*, 21−25.
33. Tsang, S. S., Muniyappa, K., Azhderian, E., Gonda, D., Radding, C. M., Flory, J., and Chase, J. (1985) *J. Mol. Biol. 185*, 295−309.
34. Kumar, R. A., Vaze, M. B., Chandra, N. R., Vijayan, M., and Muniyappa, K. (1986) *Biochemistry 35*, 1793−1803.
35. Maxam, A. M., and Gilbert, W. (1980) *Methods Enzymol. 65*, 499−560.
36. Leahy, M. C., and Radding, C. M. (1986) *J. Biol. Chem. 261*, 695−660.
37. Hsieh, P., Camerini-Otero, C. S., and Camerni-Otero, R. D. (1992) *Proc. Natl. Acad. Sci. U.S.A. 89*, 6492−6496.
38. Sibenaller, Z. A., Sorensen, B. R., and Wold, M. S. (1998) *Biochemistry 37*, 12496−12506.
39. Lao, Y., Lee, C. G., and Wold, M. S. (1999) *Biochemistry 38*, 3974−3984.
40. Blakesley, R. W., Dodgsen, J. B., Nes, I. F., and Wells, R. D. (1977) *J. Biol. Chem. 252*, 7300−7306.
41. Iida, S., and Hayatsu, H. (1971) *Biochim. Biophys. Acta 240*, 370−375.
42. Leroy, J. L., Kochoyan, M., Huynh-Dinh, T., and Gueron, M. (1988) *J. Mol. Biol. 200*, 223−238.
43. Gupta, R. C., Folta-Stogniew, E., O'Malley, S., Takahashi, M., and Radding, M. (1999) *Mol. Cell 4*, 705−714.
44. Krauss, G., Sindermann, U., Schomburg, U., and Mass, G. (1981) *Biochemistry 20*, 5346−5352.
45. Beernink, H. T. T and Morrical, S. W. (1999) *Trends Biochem. Sci. 24*, 385−389.
46. Umezu, K., Chi, N. W., and Kolodner, R. D. (1993) *Proc. Natl. Acad. Sci. U.S.A. 90*, 3875−3879.
47. Shan, Q., Bork, J. M., Webb, B. L., Inman, R. B., and Cox, M. M. (1997) *J. Mol. Biol. 265*, 519−540.
48. Umezu, K., and Kolodner, R. D. (1994) *J. Biol. Chem. 269*, 30005−30013.
49. Webb, B. L., Cox, M. M., and Inman, R. B. (1997) *Cell 91*, 347−256.
50. Register, J. C., III, and Griffith, J. (1985) *J. Biol. Chem. 260*, 12308−12312.
51. Lindsley, J. E., and Cox, M. M. (1989) *J. Mol. Biol. 205*, 695−711.
52. Konforti, B. B., and Davis, R. W. (1991) *J. Biol. Chem. 266*, 1012−10121.
53. Konforti, B. B., and Davis, R. W. (1991) *Cell 66*, 361−371.
54. Nishinaka, T., Shinohara, A., Ito, Y., Yokoyama, S., and Shibata, T. (1998) *Proc. Natl. Acad. Sci. U.S.A. 95*, 11071−11076.
55. Bertucat, G., Lavery, R., and Prevost, C. (1999) *Biophys. J. 77*, 1562−1576.
56. Schmellik-Sandage, C. S., and Tessman, E. S. (1990) *J. Bacteriol. 172*, 4378−4385.
57. Kang, S., Jaworski, A., Ohshima, K., and Wells, R. D. (1995) *Nat. Genet. 10*, 213-218.
58. Freudenreich, C. H., Stavenhagen, J. B., and Zakian, V. A. (1997) *Mol. Cell. Biol. 17*, 2090−2098.
59. Gacy, A. M., Goellner, G. M., Spiro, C., Chen, X., Gupta, G., Bradbury, E. M., Dyer, R. B., Mikesell, M. J., Yao, J. Z., and Johnson et al. (1998) *Mol. Cell 1*, 583−596.
60. Miret, J. J., Pessoa-Brandao, L., and Lahue, R. S. (1998) *Proc. Natl. Acad. Sci. U.S.A 95*, 12438−12443.
61. Kang, S., Ohshima, K. Shimizu, M., Amirrhaeri, S., and Wells, R. D. (1995) *J. Biol. Chem. 270*, 27014−2021.
62. Nag, D. K., White, M. A., and Petes, T. D. (1989) *Nature 340*, 318−320.
63. Moore, H., Greenwell, P. W., Liu, C., Arnheim, N., and Petes, T. D. (1999) *Proc. Natl. Acad. Sci. U.S.A. 96*, 1504−1509.
64. Spiro, C., Pelletier, R., Rolfsmeier, M. L., Dixon, M. J., Lahue, R. S., Gupta, G., Park, M. S., Chen, X., Mariappan, S. V., and McMurray, C. T. (1999) *Mol. Cell 4*, 1079−1085.
65. Kokoska, R. J., Stefanovic, L., Tran, H. T., Resnick, M. A., Gordenin, D. A., and Petes, T. D. (1998) *Mol. Cell. Biol. 18*, 2779−2788.
66. Tishkoff, D. X., Filosi, N., Gaida, G. M., and Kolodner, R. D. (1997) *Cell 88*, 253−263.
67. Clore, M. G., Gronenborn, A. M., Greipel, J., and Maas, G. (1986) *J. Mol. Biol. 187*, 119−124.

BI001187+